

# Regulation of the Kv2.1 Potassium Channel by MinK and MiRP1

Zoe A. McCrossan · Torsten K. Roepke ·  
Anthony Lewis · Gianina Panaghie ·  
Geoffrey W. Abbott

Received: 24 September 2008 / Accepted: 13 January 2009 / Published online: 14 February 2009  
© Springer Science+Business Media, LLC 2009

**Abstract** Kv2.1 is a voltage-gated potassium (Kv) channel  $\alpha$ -subunit expressed in mammalian heart and brain. MinK-related peptides (MiRPs), encoded by *KCNE* genes, are single-transmembrane domain ancillary subunits that form complexes with Kv channel  $\alpha$ -subunits to modify their function. Mutations in human MinK (*KCNE1*) and MiRP1 (*KCNE2*) are associated with inherited and acquired forms of long QT syndrome (LQTS). Here, coimmunoprecipitations from rat heart tissue suggested that both MinK and MiRP1 form native cardiac complexes with Kv2.1. In whole-cell voltage-clamp studies of subunits expressed in CHO cells, rat MinK and MiRP1 reduced Kv2.1 current density three- and twofold, respectively; slowed Kv2.1 activation (at +60 mV) two- and threefold, respectively; and slowed Kv2.1 deactivation less than twofold. Human MinK slowed Kv2.1 activation 25%, while human MiRP1 slowed Kv2.1 activation and

deactivation twofold. Inherited mutations in human MinK and MiRP1, previously associated with LQTS, were also evaluated. D76N–MinK and S74L–MinK reduced Kv2.1 current density (threefold and 40%, respectively) and slowed deactivation (60% and 80%, respectively). Compared to wild-type human MiRP1–Kv2.1 complexes, channels formed with M54T– or I57T–MiRP1 showed greatly slowed activation (tenfold and fivefold, respectively). The data broaden the potential roles of MinK and MiRP1 in cardiac physiology and support the possibility that inherited mutations in either subunit could contribute to cardiac arrhythmia by multiple mechanisms.

**Keywords** Potassium channel · Long QT syndrome · *KCNE1* · *KCNE2*

## Abbreviations

ERG	<i>ether-a-go-go</i> related gene product
Kv channel	Voltage-gated potassium channel
MiRP	MinK-related peptide
TEA	Tetraethylammonium
TM	Transmembrane

Z. A. McCrossan and T. K. Roepke have contributed equally to this work.

**Electronic supplementary material** The online version of this article (doi: 10.1007/s00232-009-9154-8) contains supplementary material, which is available to authorized users.

Z. A. McCrossan · T. K. Roepke · A. Lewis · G. Panaghie ·  
G. W. Abbott (✉)

Greenberg Division of Cardiology, Departments of Medicine and Pharmacology, Weill Medical College of Cornell University, Starr 463, 1300 York Avenue, 10065 New York, NY, USA  
e-mail: gwa2001@med.cornell.edu

## Present Address:

T. K. Roepke  
Charite Campus Berlin-Buch, Experimental and Clinical Research Center, Franz Volhard Clinic and HELIOS Klinikum, Berlin-Buch, Berlin, Germany

## Introduction

Voltage-gated potassium (Kv) channel pore-forming  $\alpha$ -subunits open in response to cellular depolarization to allow outward  $K^+$  ion diffusion, mediating cellular repolarization. *KCNE* genes encode single-transmembrane domain ancillary peptides termed “MinK-related peptides,” or MiRPs. MiRPs form complexes with Kv channel  $\alpha$ -subunits to modulate their function, helping generate the

broad array of Kv currents observed in excitable cells. MinK (*KCNE1*) and MiRPs 1–4 (*KCNE2-5*) transcripts have all been detected in human heart (Abbott et al. 1999; Chen et al. 2003; Piccini et al. 1999). MinK associates with the KCNQ1 Kv channel  $\alpha$ -subunit to form the  $I_{K_s}$  ventricular repolarization current in human heart; MiRP1 modulates the human *ether-a-go-go*-related gene product (hERG)  $\alpha$ -subunit, which forms the cardiac  $I_{K_r}$  repolarization current in human heart. Inherited mutations in human MinK, MiRP1, KCNQ1 and hERG account for four variants of inherited long QT syndrome (LQTS), and MiRP1 mutations are also associated with acquired LQTS (Sesti et al. 2000). The known partnering promiscuity of MiRPs in heterologous expression experiments raises the possibility that MinK and MiRP1 might perform multiple roles in the heart and other tissues.

Kv2.1 is a delayed rectifier potassium channel ubiquitously expressed in the brain, where it controls excitability in a wide range of mammalian neurons (Antonucci et al. 2001; Du et al. 1998; Frech et al. 1989; Murakoshi and Trimmer 1999). Kv2.1 is also widely expressed in rodent heart (Bou-Abboud et al. 2000; Dixon and McKinnon 1994; Xu et al. 1999a, b) and is reported to contribute to both  $I_{K_{slow}}$  in mouse ventricles and its equivalent current in murine atria ( $I_{K_s}$ ), as well as  $I_{ss}$  in mouse atria (Bou-Abboud et al. 2000; Bou-Abboud and Nerbonne 1999). Kv2.1 protein has been detected in human atria (Van Wagoner et al. 1997), and Kv2.1 mRNA is present in human ventricle (Kaab et al. 1998); but to date, Kv2.1 lacks a known native current correlate in human heart. In the rat heart Kv2.1 expression is higher in the atrial membranes than in the ventricles (Barry et al. 1995) and Kv2.1 expression is downregulated in models of cardiac hypertrophy (Capuano et al. 2002), myocardial infarction (Huang et al. 2001) and hypothyroidism (Le Bouter et al. 2003).

The functional diversity of Kv2.1 current properties is increased by its ability to associate with a variety of accessory subunits. Modulatory subunits for Kv2.1 include electrically silent Kv  $\alpha$ -subunits such as Kv5.1, Kv6.1 (Post et al. 1996), Kv8.1 (Salinas et al. 1997a), Kv9.1–9.3 (Salinas et al. 1997b) and the KChAP ancillary subunit (Kuryshv et al. 2000). While silent Kv  $\alpha$ -subunits serve to increase the functional diversity of current kinetics by assembling with Kv2.1 subunits to form heterotetrameric channels at the cell surface (all subunits lining the pore), KChAP is cytoplasmic and associates at the intracellular amino terminus of Kv2.1 to produce a significant increase in both Kv2.1 channel protein and the number of functional channels at the cell surface (Kuryshv et al. 2000). We previously showed that MiRP2 forms complexes with Kv2.1 in rat brain and that in Chinese hamster ovary (CHO) cell coexpression studies, MiRP2 slows Kv2.1

activation and deactivation and increases the extent of inactivation (McCrossan et al. 2003). We also recently generated a *kcne2* null mouse to examine the native roles of MiRP1 (KCNE2). We found that in murine ventricles MiRP1 coassembles with and functionally regulates Kv1.5 and Kv4.2 but not Kv2.1 (Roepke et al. 2008). The findings of these latter two studies led us to examine whether MinK and MiRP1 were capable of forming complexes with Kv2.1 in vitro or in vivo in other animal models and what the functional effects might be.

Here, using native coimmunoprecipitations, we detected native MinK–Kv2.1 and MiRP1–Kv2.1 complexes in rat heart tissue and found that rat and human MinK and MiRP1 modify the gating properties of Kv2.1 channels heterologously expressed in CHO cells. Mutations in human MinK and MiRP1 are thought to underlie LQTS via effects on complexes formed with either KCNQ1 or hERG  $\alpha$ -subunits; here, we show that mutations in human MinK and MiRP1 previously associated with inherited LQTS also alter the function of channels formed with Kv2.1. This raises the possibility that MinK or MiRP1 mutations may contribute to cardiac dysfunction via impairment of the function of cardiac channel complexes formed with Kv2.1. Further, the formation of MinK–Kv2.1 complexes in vivo could explain the recent findings that *kcne1* null mice exhibit atrial fibrillation and that these mice show increased atrial myocyte  $I_K$  compared to wild-type (Temple et al. 2005), a result inconsistent with effects on  $I_{K_s}$  because MinK upregulates KCNQ1 current (Barhanin et al. 1996; Sanguinetti et al. 1996; Sesti and Goldstein 1998).

## Methods

### RT-PCR

Kv2.1, MinK, MiRP1 and MiRP2 RNA expression was detected by RT-PCR. For all native tissue studies in this report, adult Sprague-Dawley rats were housed and utilized according to the NIH *Guide for the Care and Use of Laboratory Animals* and Weill Medical College of Cornell University animal care and use policies and humanely killed by CO<sub>2</sub> inhalation prior to tissue extraction. Hearts were removed and rinsed, then the tissue was frozen and disrupted under liquid nitrogen using a RNA-zap-treated mortar and pestle. The frozen tissue was homogenized through a Qiashredder (Qiagen, Valencia City, CA). Total RNA was extracted from homogenized samples using the RNeasy kit (Qiagen), cleaned with DNase I using the on-column RNase-free kit (Qiagen) and reverse-transcribed using the Superscript II first-strand synthesis kit (Invitrogen, Carlsbad, CA). Primer sequences were as follows (5′–3′): rKv2.1, AGGCCGAACTGTGTCTACTC (sense)

and GTCCTCTGCACCCTCCTAAC (antisense) (Conforti and Millhorn 1997); rMinK, CACAAGTGTCTGCCTTTCTG (sense) and TTCATGACAGTGGCTTCAGTTC (antisense); rMiRP1, AGGGGAAACATGACCACTT (sense) and GCAGATGGACTCTCGTTCTT (antisense); rMiRP2, CAGATCGCAGAGTCAGTTTCTAGC (sense) and TCGAGATGAGTTCCGGAGACC (antisense), giving PCR products of 557, 376, 403 and 596 bp, respectively. Gene identities were confirmed by sequencing single bands cut from 1% agarose gels.

#### Western Blotting and Coimmunoprecipitation

Protocols for preparation of crude heart plasma membranes and immunoprecipitations were adapted from previous protocols (McCrossan et al. 2003; Pitts 1979). Frozen whole hearts from adult Sprague-Dawley rats were homogenized, resuspended in 5 ml buffer (per three hearts)—comprising (in mM) 0.6 sucrose, 10 3-(*N*-morpholino)propanesulfonic acid (MOPS) plus protease inhibitor cocktail (Boehringer-Mannheim, Mannheim, Germany), pH 7.4—and centrifuged for 5 min at 500*g*. This and all following centrifugation steps were carried out at 4°C. The supernatant was recentrifuged for 30 min at 12,000*g*, the pellet discarded and the supernatant diluted to 40 ml with buffer comprising (in mM) 160 NaCl, 20 MOPS plus protease inhibitors, pH 7.4. Then, 10 ml of 1 M sucrose was added and the solution centrifuged for 1 h at 160,000*g*. The resulting pellet was resuspended in buffer comprising (in mM) 54 LiCl, 6 KCl, 100 NaCl, 20 MOPS plus protease inhibitors, pH 7.4; homogenized by passing through progressively smaller-gauge syringe needles; then diluted 10:1 with immunoprecipitation (IP) buffer, comprising (in mM) 150 NaCl, 50 Tris-HCl (pH 7.4), 20 NaF, 10 NaVO<sub>4</sub> and 1 phenylmethylsulfonyl fluoride (Fisher Scientific, Fair Lawn, NJ), as well as 1% Nonidet P-40 (Pierce, Rockford, IL), 1% 3-[(3-cholamidopropyl)dimethyl-ammonio]1-propane sulfonate (CHAPS; Sigma, St. Louis, MO), 1% Triton X-100 (Fisher Scientific) and 0.5% SDS (Sigma). The mixture was incubated on a rocking platform for 1 h at 4°C, debris removed by centrifugation at 20,000*g* for 5 min and the supernatant retained. The supernatant was precleared by incubation with Protein A-Sepharose 4B beads (Pierce) for 30 min, the beads being removed by centrifugation.

The precleared supernatant was incubated with antibodies for immunoprecipitation: anti-Kv2.1 (Sigma), anti-ERG (Sigma), anti-A1 adenosine receptor (A1-R; Santa Cruz Biotechnology, Santa Cruz, CA) or in-house rabbit polyclonal antibodies raised against MinK, MiRP1 or MiRP2, for 2–16 h at 4°C. Protein A-Sepharose 4B beads were then added, and the mixture was incubated for a further 5 h at 4°C. The complexed beads were collected by

centrifugation and washed in IP buffer for 4 × 20 min, and then purified complexes were eluted by incubating the beads for 20 min at 37°C in 5% β-mercaptoethanol, 1 mM EDTA, 1.5% SDS and 10% glycerol in 50 mM Tris buffer, pH 6.7. Postcentrifugation, the resulting bead eluates were heated for a further 20 min at 50°C and then size-fractionated by SDS-PAGE. Following membrane transfer, blots were probed with primary antibodies as indicated and detected with goat anti-rabbit horseradish peroxidase-coupled secondary antibodies (Bio-Rad, Richmond, CA) for fluorography. Western blots were also performed directly on crude membrane fractions, to detect expression of subunits in rat heart membrane fractions, and on lysates from nontransfected CHO cells and CHO cells transfected with expression plasmids for rat MinK, MiRP1 or MiRP2 (see below).

#### Cell Culture, Transfection and Immunofluorescence Analysis

CHO cells were cultured as previously described (McCrossan et al. 2003) and cotransfected with expression vectors containing cDNA encoding rat Kv2.1, GFP and wild-type rat or human variants of MinK, MiRP1 or human mutants (hMinK-D76N, hMinK-S74L, hMiRP1-M54T, hMiRP1-I57T). Standard Superfect (Qiagen) transfection protocols were used; then, cells were plated on glass coverslips for 24 h to allow for gene expression before whole-cell recordings, protein biochemistry or immunofluorescence analysis. Immunofluorescence analysis of Kv2.1 and HA-tagged rat MinK and MiRP1 localization was performed as previously described (McCrossan et al. 2003).

#### Electrophysiology

Whole-cell patch-clamp recordings of CHO cells expressing subunits as described above were performed at 22–25°C using an IX50 inverted microscope equipped with epifluorescence optics for GFP detection (Olympus, Tokyo, Japan), a Multiclamp 700A Amplifier, a Digidata 1300 Analogue/Digital converter and a PC with pClamp9 software (Axon Instruments, Foster City, CA). CHO cells were bathed in a physiological solution comprising (in mM) 135 NaCl, 5 KCl, 1.2 MgCl<sub>2</sub>, 5 HEPES, 2.5 CaCl<sub>2</sub> and 10 D-glucose (pH 7.4). Borosilicate glass pipettes (Sutter, Novato, CA) were of 3–5 MΩ resistance when filled with intracellular solution containing (in mM) 10 NaCl, 117 KCl, 2 MgCl<sub>2</sub>, 11 HEPES, 11 EGTA and 1 CaCl<sub>2</sub> (pH 7.2). Cells were stepped from a holding potential of –80 mV to test potentials between –60 and +60 mV in 10-mV increments for 2 s duration, followed by a tail pulse to –40 mV for 1 s duration, repeated at 0.1 Hz. Leak and

liquid junction potentials (<4 mV) were not compensated for when generating current–voltage relationships. Conductance–voltage relationships were determined by plotting tail currents vs. prepulse voltage. Normalized conductance–voltage relationships were fit with a Boltzmann function,  $G = G_{max}/[1 + \exp(V - V_{0.5}/k)]$ , where  $V_{0.5}$  is the half-maximal activation and  $k$  is the slope factor. Tetraethylammonium (TEA) dose responses were fit with a logistic dose–response function,  $y = [A_1 - A_2/1 + (x_0/x)^p] + A_2$ , where  $x_0$  is the half-maximal inhibition and  $p$  is the slope factor. Data were analyzed using pClamp9 software, and statistical analysis (one-way ANOVA) was performed using Origin 6.1 (Microcal, Northampton, MA) software. Error bars on figures indicate standard error of the mean.

## Results

### Immunoprecipitation of MinK–Kv2.1 and MiRP1–Kv2.1 Complexes from Rat Heart Tissue

Kv2.1, MinK, MiRP1 and MiRP2 transcript expression in whole rat heart was detected using RT-PCR (Fig. 1a, b). In-house antibodies raised against MinK, MiRP1 and MiRP2 epitopes were shown to detect rat MinK, MiRP1 and MiRP2, respectively, in transfected CHO cells and to not detect proteins in nontransfected CHO cells (Fig. 1c). Kv2.1, ERG, MinK, MiRP1 and MiRP2 proteins were also detected in rat heart membrane fractions using their respective antibodies (Fig. 1d). The multiple bands observed here in some cases for MiRPs are consistent with previous reports of several glycosylated or unglycosylated forms of MiRP subunits being detectable in heterologous or native preparations (Abbott et al. 1999, 2001). Similarly, each  $\alpha$ -subunit showed two main bands corresponding to monomeric and multimeric forms and minor bands presumed to be immature (nonglycosylated) forms.

Immunoprecipitations from rat heart membrane fractions were performed with antibodies raised against Kv2.1, A1-R, MinK, MiRP1 or MiRP2. The resultant immunoprecipitates were size-fractionated and Western-blotted to detect coimmunoprecipitated proteins. Kv2.1 protein was immunoprecipitated from rat heart membranes with anti-Kv2.1, anti-MinK and anti-MiRP1 antibodies ( $n = 4$ ) but not with anti-A1-R or anti-MiRP2 antibodies ( $n = 2$ ) (Fig. 1e). MinK was coimmunoprecipitated from rat heart membranes with anti-Kv2.1, anti-ERG and anti-MinK antibodies ( $n = 2$ ) (Fig. 1f, upper). MiRP1 was coimmunoprecipitated from rat heart membranes with anti-Kv2.1, anti-ERG and anti-MiRP1 antibodies ( $n = 2$ ) (Fig. 1f, lower). In summary, the data suggest that MinK and MiRP1, but not MiRP2, form stable complexes with Kv2.1 and with ERG in rat heart membranes.

### Rat MinK and MiRP1 Alter Kv2.1 Gating in CHO Cell Expression Studies

Cloned Kv2.1 was heterologously expressed with rat MinK or MiRP1 in CHO cells and functional effects quantified using whole-cell voltage-clamp recording. Untransfected CHO cells showed no significant whole-cell currents; neither did cells transfected with MinK or MiRP1 alone (data not shown). Transfection of CHO cells with Kv2.1 alone gave moderately fast activating and deactivating, slow inactivating outward currents at depolarized voltages, as previously reported (Frech et al. 1989) (Fig. 2a). Coexpression with rat MinK reduced mean Kv2.1 current density approximately twofold ( $P < 0.001$  at 20–60 mV,  $n = 14–42$ ) (Fig. 2a, b), without altering the conductance–voltage relationship (data not shown). Figure 2c shows normalization of early (300 ms) portions of traces, demonstrating activation to peak at 0 mV. Fitting of activation to peak with a single exponential for each voltage gave an approximation of the time constant of activation ( $\tau$ ). Rat MinK produced approximately twofold slowing of Kv2.1 activation (at 60 mV:  $P < 0.05$ ,  $n = 14–42$ ) (Fig. 2c, d). Figure 2e shows exemplar traces of deactivation of Kv2.1 alone or with rat MinK at –40 mV in CHO cells. Deactivation at –40 mV was fitted with a double exponential function, revealing that rat MinK slowed both components of Kv2.1 deactivation ( $\tau_{slow}$ , Kv2.1 alone,  $119 \pm 9$  ms; Kv2.1–rMinK,  $201 \pm 33$  ms;  $\tau_{fast}$ , Kv2.1 alone,  $17 \pm 1$  ms; Kv2.1–rMinK,  $23 \pm 1$  ms;  $P < 0.05$ ) with a small decrease in the relative amplitude of the slow component of Kv2.1 deactivation (Kv2.1 alone,  $0.49 \pm 0.02$  ms; Kv2.1–rMinK,  $0.34 \pm 0.03$  ms;  $P < 0.05$ ) (Fig. 2e–g). Rat MiRP1 had qualitatively similar effects on Kv2.1: a threefold reduction in mean current density (Fig. 2a, b) and a marked slowing of activation, threefold at +60 mV ( $P < 1 \times 10^{-7}$ ,  $n = 17–19$ ) (Fig. 2c, d). Rat MiRP1 also increased the  $\tau$  of the slow component of Kv2.1 deactivation by 50% ( $P < 0.001$ ,  $n = 17–19$ ) without altering its relative amplitude compared to Kv2.1 alone (Fig. 2e–g). The altered gating of Kv2.1 when coexpressed with rat MinK or MiRP1 suggested the formation of heteromeric channel complexes at the plasma membrane in CHO cells. This was supported by immunofluorescence studies which showed colocalization of Kv2.1 with rat MinK and with rat MiRP1 at the cell surface (Supplementary Fig. 1).

### Human MiRP1 and MinK Alter Kv2.1 Gating in CHO Cell Expression Studies

We and others previously demonstrated MinK and MiRP1 species-dependent effects (McCrossan and Abbott 2004); therefore, we next examined the functional effects of human MinK and MiRP1 on Kv2.1 using whole-cell



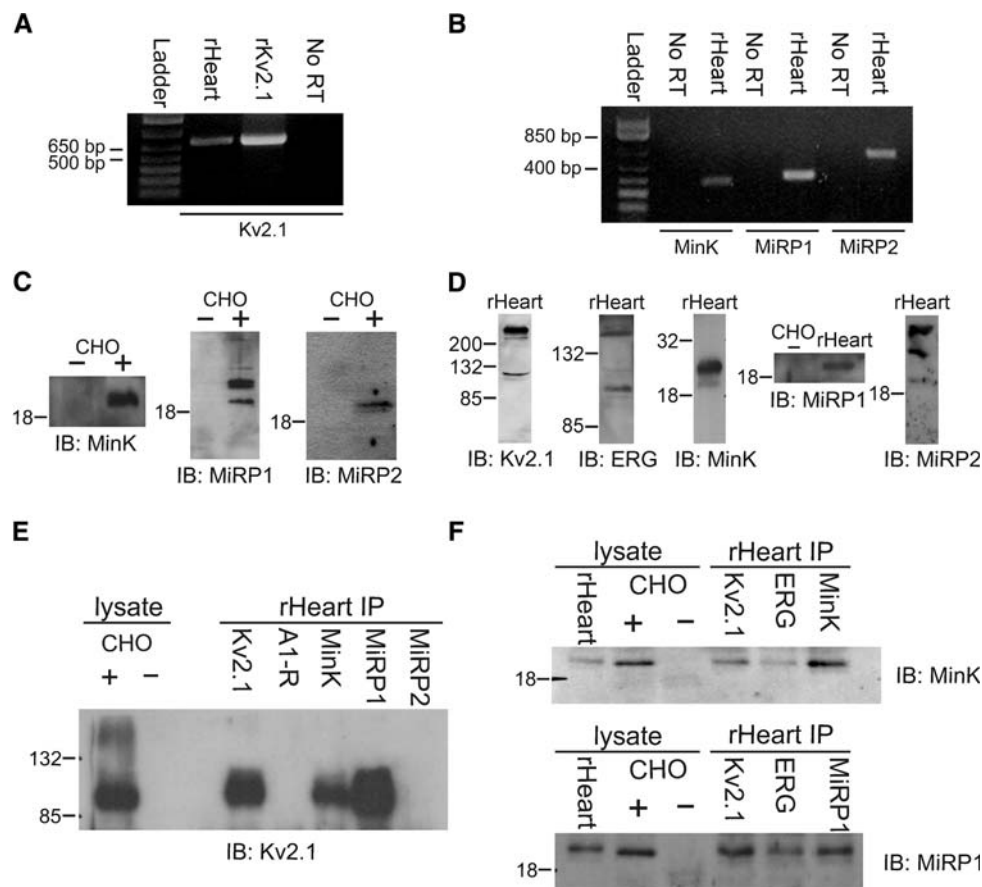


**Fig. 1** Immunoprecipitation of MinK–Kv2.1 and MiRP1–Kv2.1 complexes from rat heart. **a** RT-PCR indicating expression of Kv2.1 mRNA in rat heart. Markers indicate migration of DNA ladder markers on agarose gel. mRNA was extracted from rat heart and cDNA was produced by reverse transcription, then amplified by Kv2.1-specific primers. Lanes: rHeart, cDNA amplified from rat heart mRNA; rKv2.1, positive control using Kv2.1 cDNA in a plasmid; No RT, as for rHeart lane but without reverse transcription (negative control). **b** RT-PCR showing expression of MinK, MiRP1 and MiRP2 mRNA in rat heart. Markers indicate migration of DNA ladder markers on agarose gel. Lanes: rHeart, cDNA amplified from rat heart mRNA with primers as indicated; No RT, as for rHeart lanes but without reverse transcription (negative controls). **c** Western blot analysis of MinK, MiRP1 and MiRP2 in CHO cells transfected with expression plasmids containing cDNA for MinK, MiRP1 or MiRP2, respectively. –, nontransfected CHO cell lysate (negative control); +, lysates from CHO cells transfected with MinK, MiRP1 or MiRP2, as indicated by the antibody used for immunoblotting (IB, lower labels). Numbered labels to left of each blot indicate migration of molecular weight markers (in kD) on SDS-PAGE gel. **d** Western blot analysis of native channel subunit expression in rat heart membrane fractions. Lanes: –, nontransfected CHO cell lysate (negative control); rHeart, membrane fraction from rat heart. Lower labels indicate antibody used for immunoblotting (IB). Numbered labels to left of each blot

indicate migration of molecular weight markers (in kD) on SDS-PAGE gel. **e** Native coimmunoprecipitations of channel subunits from rat heart membrane fractions. Exemplar Western blot using anti-Kv2.1 antibody for immunoblotting (IB) of Kv2.1 in Kv2.1-transfected CHO cell lysate and in rat heart membrane fractions (rHeart IP) immunoprecipitated by antibodies raised against Kv2.1, MinK or MiRP1 ( $n = 4$  experiments). Kv2.1 was not detected in nontransfected CHO cell lysate or in rat heart membrane fractions immunoprecipitated by antibodies raised against the A1 adenosine receptor (A1-R) or MiRP2 ( $n = 2$  experiments). Numbered labels to left of each blot indicate migration of molecular weight markers (in kD) on SDS-PAGE gel. **f** Reciprocal native coimmunoprecipitations of channel subunits from rat heart membrane fractions. Western blots using anti-MinK (*upper gel*) or anti-MiRP1 (*lower gel*) antibodies for immunoblotting (IB). MinK was present in rat heart membranes, MinK-transfected (+) CHO cell lysate and rat heart membrane fractions (rHeart IP) immunoprecipitated by antibodies raised against Kv2.1, MinK or ERG ( $n = 2$  experiments). MiRP1 was present in rat heart membranes, MiRP1-transfected (+) CHO cell lysate and rat heart membrane fractions (rHeart IP) immunoprecipitated by antibodies raised against Kv2.1, MiRP1 or ERG ( $n = 2$  experiments). Neither subunit was detected in nontransfected CHO cell lysate. Numbered labels to left of each blot indicate migration of molecular weight markers (in kD) on SDS-PAGE gel

voltage clamp of transfected CHO cells. Cotransfection of human MinK or MiRP1 significantly altered neither mean Kv2.1 current density (Kv2.1,  $1,182 \pm 123$  A/F,  $n = 42$ ; Kv2.1–hMinK,  $1,022 \pm 150$  A/F,  $n = 24$ ; Kv2.1–hMiRP1,  $846 \pm 120$  A/F,  $n = 16$ ) (Fig. 3a, b) nor the Kv2.1

conductance–voltage relationship (Fig. 3c). In contrast, both subunits slowed Kv2.1 activation, hMiRP1 having significant effects at all positive voltages and hMinK at +60 mV only (Fig. 3d, e). Thus, the  $\tau$  of Kv2.1 activation at +60 mV was doubled by human MiRP1 and increased

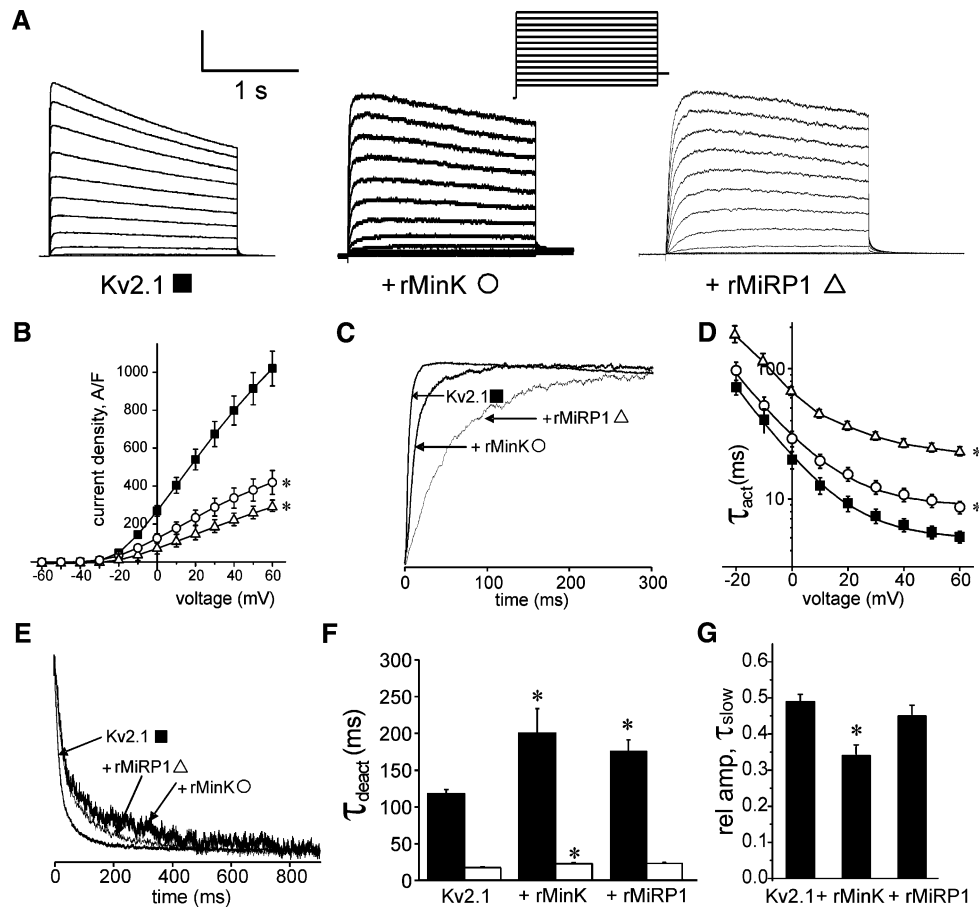


**Fig. 2** Modulation of Kv2.1 by rat MinK and MiRP1. **a** Exemplar traces showing currents recorded from CHO cells transfected with Kv2.1 alone or cotransfected with rat MinK or MiRP1 as indicated. *Insets: left, scale bars; right, voltage protocol.* Vertical scale: 2 nA, Kv2.1; 1 nA, rMiRP1-Kv2.1; 0.5 nA, rMinK-Kv2.1. **b** Mean peak current density from CHO cells transfected with Kv2.1 alone (*filled squares*,  $n = 61$ ) or cotransfected with rMinK (*circles*,  $n = 14$ ) or rMiRP1 (*triangles*,  $n = 17$ ). \*Statistical significance vs. Kv2.1 alone,  $P < 0.05$ . **c** Normalized exemplar traces showing expanded view of Kv2.1, rMinK-Kv2.1 and rMiRP1-Kv2.1 activation at 0 mV. **d** Mean activation rates of Kv2.1, rMinK-Kv2.1 and rMiRP1-Kv2.1 channels at activation voltages between  $-20$  and  $+60$  mV, fitted with a single

exponential function, expressed as  $\tau_{act}$ . \*Statistical significance vs. Kv2.1 alone,  $P < 0.05$ . Cells and symbols as in **(b)**. **e** Normalized exemplar traces showing expanded view of Kv2.1, rMinK-Kv2.1 and rMiRP1-Kv2.1 deactivation at  $-40$  mV. **f** Mean deactivation rates of Kv2.1, rMinK-Kv2.1 and rMiRP1-Kv2.1 currents at  $-40$  mV fitted with a double exponential function, showing slow (*black*) and fast (*white*)  $\tau_{deact}$  components. \*Statistical significance vs. Kv2.1 alone,  $P < 0.05$ . **g** Mean fractional amplitude of the slow component of deactivation rates of Kv2.1, rMinK-Kv2.1 and rMiRP1-Kv2.1 currents at  $-40$  mV fitted with a double exponential function. \*Statistical significance vs. Kv2.1 alone,  $P < 0.05$

25% by human MinK ( $P < 0.01$ ,  $n = 16-42$  cells). Human MiRP1 caused a twofold slowing of both components of Kv2.1 deactivation at  $-40$  mV ( $P < 0.05$ ,  $n = 16-42$  cells), whereas human MinK had no significant effect on the  $\tau$  values ( $\tau_{slow}$ , Kv2.1 alone,  $119 \pm 9$  ms; Kv2.1-hMinK,  $106 \pm 7$  ms; Kv2.1-hMiRP1,  $208 \pm 20$  ms;  $\tau_{fast}$ , Kv2.1 alone,  $17 \pm 1$  ms; Kv2.1-MinK,  $16 \pm 1$  ms; Kv2.1-hMiRP1,  $32 \pm 2$  ms) (Fig. 3f, g). Human MinK produced a small but statistically significant ( $P < 0.05$ ) increase in the relative amplitude of the slow component of deactivation, whereas hMiRP1 had no significant effect on amplitude (Kv2.1 alone,  $0.49 \pm 0.02$ ; Kv2.1-hMinK,  $0.58 \pm 0.04$ ; Kv2.1-hMiRP1,  $0.43 \pm 0.04$ ;  $n = 16-42$

cells; Fig. 3h). Despite their effects on Kv2.1 gating, neither rat MinK nor human MiRP1 significantly altered the sensitivity of Kv2.1 to block by TEA (Supplementary Fig. 2).

#### Inherited LQTS Mutations D76N and S74L Alter MinK-Kv2.1 Function

Human MinK variants D76N and S74L are associated with inherited LQTS, and both reduce MinK-KCNQ1 ( $I_{Ks}$ ) current density by a combination of gating effects and reduced unitary conductance (Sesti and Goldstein 1998; Splawski et al. 1997a, b). Here, D76N-hMinK-Kv2.1

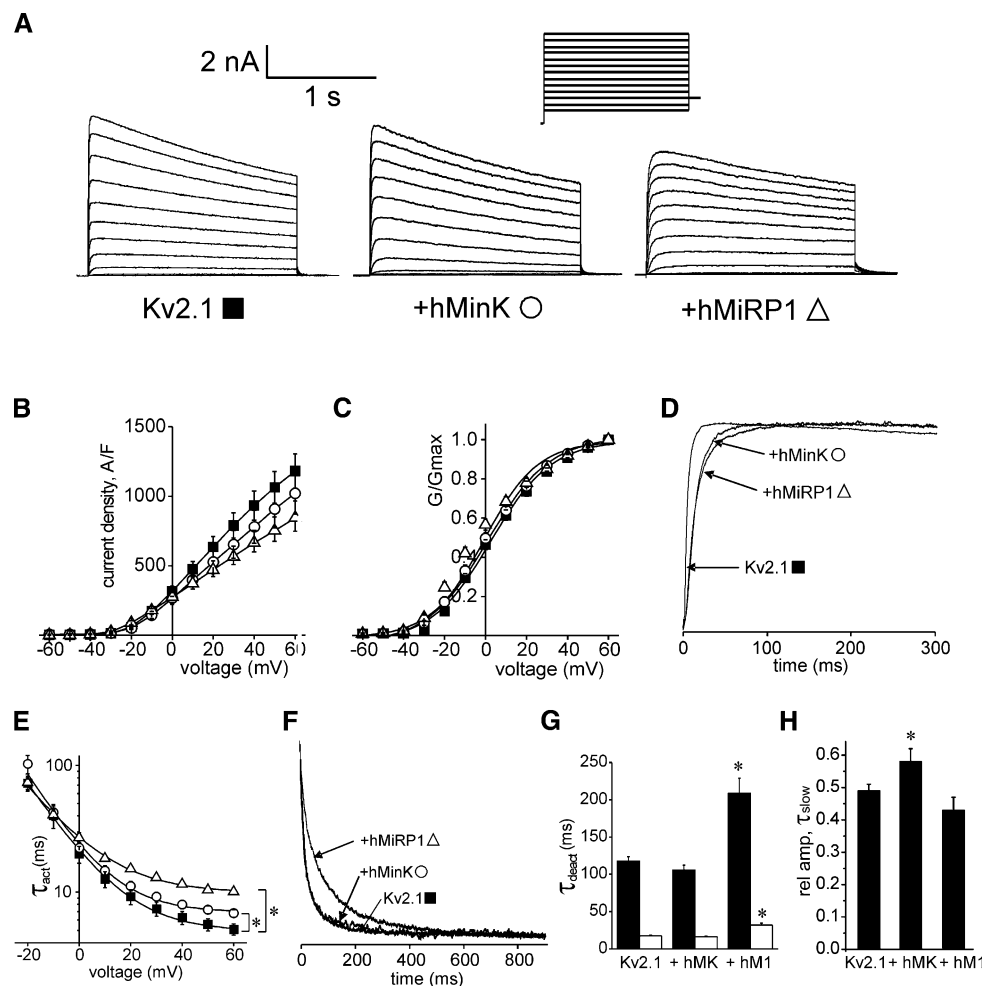


**Fig. 3** Human MinK and MiRP1 slow Kv2.1 gating. **a** Exemplar traces showing currents recorded from CHO cells transfected with Kv2.1 alone or cotransfected with human MinK or MiRP1 as indicated. *Insets: left, scale bars; right, voltage protocol.* **b** Mean peak current density from CHO cells transfected with Kv2.1 alone (*filled squares*,  $n = 42$ ) or cotransfected with hMinK (*circles*,  $n = 24$ ) or hMiRP1 (*triangles*,  $n = 16$ ). **c** Mean normalized conductance–voltage relationships, cells and symbols as in (**b**). Data were fit with a Boltzmann function,  $G = G_{max}/[1 + \exp(V - V_{0.5}/k)]$ , giving values for midpoint voltage dependence of activation as follows: Kv2.1,  $4.4 \pm 0.7$  mV; MinK–Kv2.1,  $1.0 \pm 1.0$  mV; MiRP1–Kv2.1,  $-0.6 \pm 0.8$  mV. Slopes were  $11.3 \pm 0.4$ ,  $15.2 \pm 0.9$  and  $13.1 \pm 0.5$  mV, respectively. **d** Normalized exemplar traces showing expanded view

of Kv2.1, hMinK–Kv2.1 and hMiRP1–Kv2.1 activation at 0 mV. **e** Mean activation rates of Kv2.1, hMinK–Kv2.1 and hMiRP1–Kv2.1 channels at activation voltages between  $-10$  and  $+60$  mV, fitted with a single exponential function, expressed as  $\tau_{act}$ . **f** Normalized exemplar traces showing expanded view of Kv2.1, hMinK–Kv2.1 and hMiRP1–Kv2.1 deactivation at  $-40$  mV. **g** Mean deactivation rates of Kv2.1, hMinK–Kv2.1 and hMiRP1–Kv2.1 currents at  $-40$  mV fitted with a double exponential function, showing slow (*black*) and fast (*white*)  $\tau_{deact}$  components. \*Statistical significance vs. Kv2.1 alone,  $P < 0.05$ . **h** Mean fractional amplitude of the slow component of deactivation rates of Kv2.1, hMinK–Kv2.1 and hMiRP1–Kv2.1 currents at  $-40$  mV fitted with a double exponential function. \*Statistical significance vs. Kv2.1 alone,  $P < 0.05$

channels showed significantly reduced current density compared to wild-type hMinK–Kv2.1 complexes, while the apparent reduction observed with S74L–MinK did not reach statistical significance (D76N–MinK–Kv2.1,  $332 \pm 104$  A/F; S74L–MinK–Kv2.1,  $708 \pm 73$  A/F; vs. hMinK–Kv2.1,  $1,022 \pm 150$  A/F) (Fig. 4a, b). Neither mutation altered the voltage dependence or rate of hMinK–Kv2.1 activation (Fig. 4c, d). Both mutations significantly increased the  $\tau$  of both components of deactivation but decreased the relative amplitude of the slow component

(Fig. 4e, f) without significantly altering inactivation (not shown).

#### Inherited LQTS Mutations I57T and M54T Impair MiRP1–Kv2.1 Activation

Human MiRP1 variants M54T and I57T are associated with inherited and acquired LQTS; M54T accelerates MiRP1–hERG deactivation, while I57T reduces MiRP1–hERG current density (Abbott et al. 1999; Sesti et al.

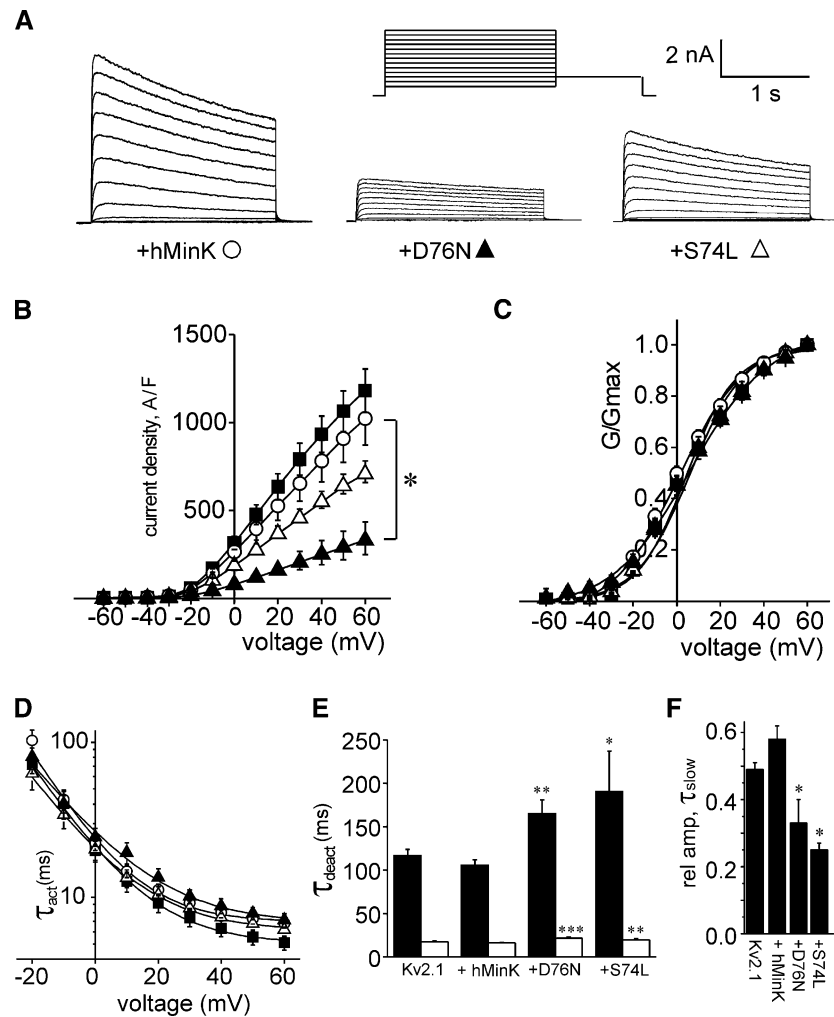


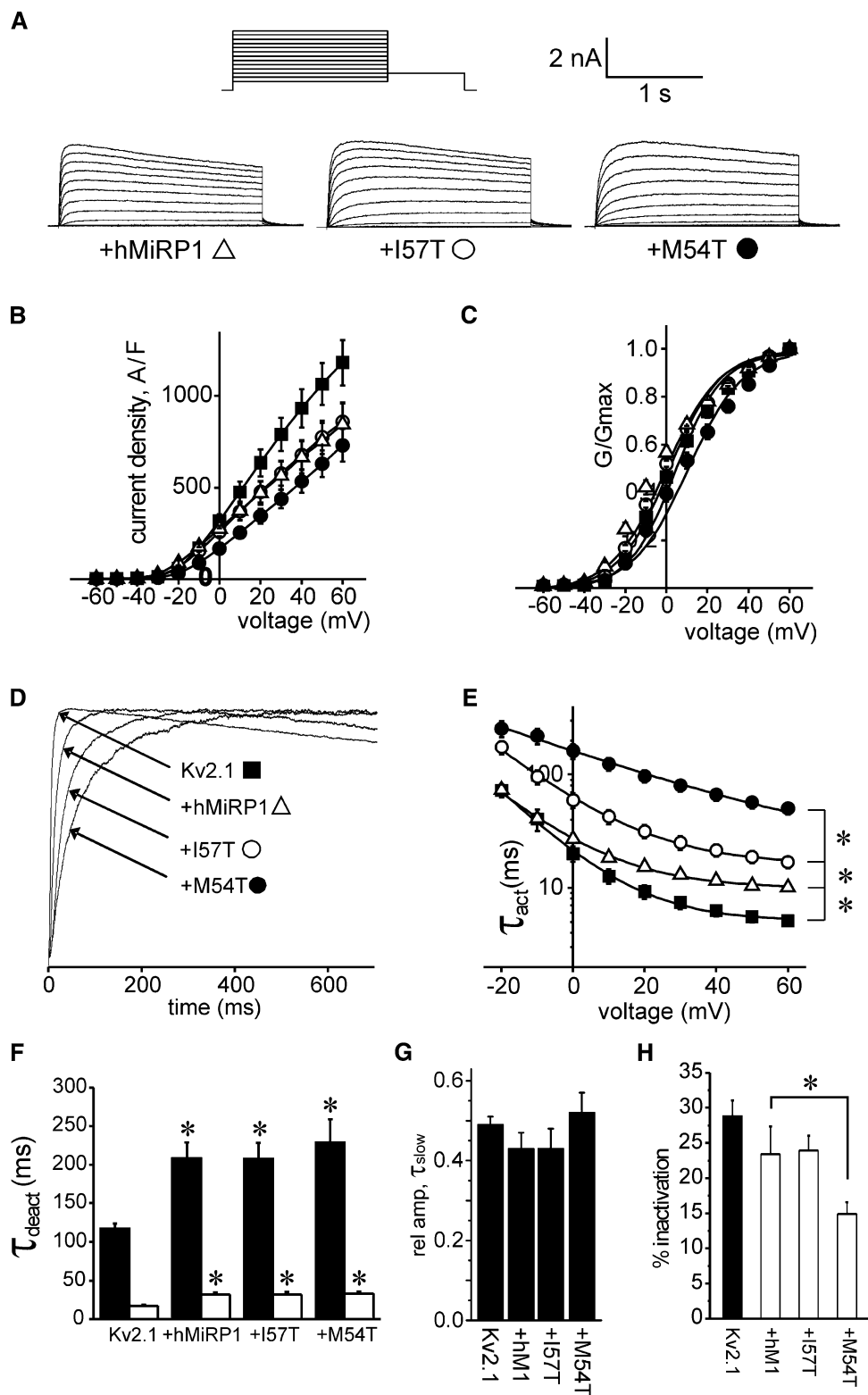
**Fig. 4** Effects of inherited human MinK mutations on MinK–Kv2.1 function. **a** Exemplar traces showing currents recorded from CHO cells cotransfected with Kv2.1 + wild-type human MinK (+hMinK), Kv2.1 + D76N–MinK (+D76N) or Kv2.1 + S74L–MinK (+S74L), as indicated. *Insets: left, voltage protocol; right, scale bars.* **b** Mean peak current density from CHO cells transfected with Kv2.1 alone (filled squares) or with wild-type (open circles,  $n = 14$ ), D76N (filled triangles,  $n = 9$ ) or S74L (open triangles,  $n = 11$ ) human MinK. \*Statistically significant difference ( $P < 0.001$ ). **c** Mean normalized conductance–voltage relationships, cells and symbols as in (b). Fitting of the data with a Boltzmann function,  $G = G_{max}/[1 + \exp(V - V_{0.5}/k)]$ , gave values for midpoint voltage dependence of activation as follows: Kv2.1,  $4.4 \pm 0.7$  mV; wild-type human MinK–Kv2.1,  $1.0 \pm 1.0$  mV; D76N–MinK–Kv2.1,  $6.0 \pm 1.6$  mV; S74L–MinK–

Kv2.1,  $6.2 \pm 0.7$  mV. Slopes were  $11.3 \pm 0.4$ ,  $15.2 \pm 0.9$ ,  $18.0 \pm 1.8$  and  $12.5 \pm 0.5$  mV, respectively. **d** Mean activation rates, cells and symbols as in (b). Activation rates at voltages between  $-10$  and  $+60$  mV were fitted with a single exponential function, expressed as  $\tau_{act}$ . **e** Mean deactivation rates for cells as in (b), subunits as indicated. Deactivation rates at  $-30$  mV were fitted with a double exponential function, showing slow (black) and fast (white)  $\tau_{deact}$  components. Statistically significant differences vs. wild-type human MinK–MinK: \* $P < 0.05$ , \*\* $P < 0.01$ , \*\*\* $P < 0.001$ . **f** Mean fractional amplitude of the slow component of deactivation rates of Kv2.1 and Kv2.1 with wild-type or mutant hMinK currents at  $-40$  mV fitted with a double exponential function. \*Statistical significance vs. Kv2.1 + wild-type MinK,  $P < 0.05$

2000). Here, neither variant reduced mean current density of hMiRP1–Kv2.1 channels (M54T,  $730 \pm 89$  A/F; I57T,  $859 \pm 100$  A/F; vs. wild-type hMiRP1–Kv2.1,  $846 \pm 120$  A/F) (Fig. 5a, b). M54T positively shifted the voltage dependence of MiRP1–Kv2.1 channels by 9 mV ( $V_{1/2}$  activation for M54T was  $10.4 \pm 1.1$  vs.  $1.1 \pm 0.4$  mV for wild-type MiRP1–Kv2.1), whereas I57T had no significant effect ( $V_{1/2}$  activation  $-0.6 \pm 0.8$  mV) (Fig. 5c).

The most prominent effect of the MiRP1 mutations was a slowing of hMiRP1–Kv2.1 activation (Fig. 5a, d). At all depolarizing voltages, the slowing of activation observed with wild-type hMiRP1 was significantly increased, with the M54T mutation having the greatest effect (wild-type hMiRP1,  $10.0 \pm 1.1$  ms; I57T,  $16.8 \pm 2.0$  ms; M54T,  $50.2 \pm 5.9$  ms at  $+60$  mV) (Fig. 5e). Neither mutant altered MiRP1–Kv2.1 deactivation kinetics (both the  $\tau$  and





the relative amplitudes of the slow and fast components were unaltered, Fig. 5f, g). Although wild-type MiRP1 did not alter Kv2.1 inactivation, there was a statistically significant reduction in the extent of inactivation by M54T

(14.9 ± 1.7% over 1 s) compared to Kv2.1 homomers (28.8 ± 2.2%,  $P < 0.001$ ), wild-type MiRP1-Kv2.1 (23.4 ± 3.9%,  $P < 0.05$ ) or I57T-MiRP1-Kv2.1 channels (23.9 ± 2.1%,  $P < 0.05$ ) (Fig. 5h).

**Fig. 5** Effects of inherited human MiRP1 mutations on MiRP1–Kv2.1 function. **a** Exemplar traces showing currents recorded from CHO cells cotransfected with Kv2.1 + wild-type human MiRP1 (+MiRP1), Kv2.1 + I57T–MiRP1 (+I57T) or Kv2.1 + M54T–MiRP1 (+M54T), as indicated. *Insets: left*, voltage protocol; *right*, scale bars. **b** Mean peak current density from CHO cells transfected with Kv2.1 alone (*filled squares*,  $n = 42$ ) or with wild-type human MiRP1 (*open triangles*,  $n = 16$ ), I57T–MiRP1 (*open circles*,  $n = 21$ ) or M54T–MiRP1 (*filled circles*,  $n = 15$ ). **c** Mean normalized conductance–voltage relationships; cells and symbols as in (b). Fitting of the data with a Boltzmann function,  $G = G_{max}/[1 + \exp(V - V_{0.5}/k)]$ , gave values for midpoint voltage dependence of activation as follows: Kv2.1,  $4.4 \pm 0.7$  mV; wild-type hMiRP1–Kv2.1,  $-0.6 \pm 0.8$  mV; M54T–MiRP1–Kv2.1,  $10.4 \pm 1.1$  mV; I57T–MiRP1–Kv2.1,  $1.1 \pm 0.4$  mV. Slopes were  $11.3 \pm 0.4$ ,  $13.1 \pm 0.5$ ,  $13.4 \pm 0.6$  and  $12.5 \pm 0.3$  mV, respectively. **d** Normalized exemplar traces showing expanded view of Kv2.1 alone or with wild-type M54T– or I57T–MiRP1 (as indicated), activation at 0 mV. **e** Mean activation rates at activation voltages between  $-10$  and  $+60$  mV, fitted with a single exponential function, expressed as  $\tau_{act}$ ; cells and symbols as in (b). **f** Mean deactivation rates at  $-30$  mV fitted with a double exponential function, showing slow (*black*) and fast (*white*)  $\tau_{deact}$  components; cells as in (b), subunits as indicated. \*Statistically significant difference vs. Kv2.1 alone ( $P < 0.05$ ). **g** Mean fractional amplitude of the slow component of deactivation rates of Kv2.1 and Kv2.1 with wild-type or mutant hMiRP1 currents at  $-40$  mV fitted with a double exponential function. **h** Percent inactivation at  $+40$  mV over the initial 1 s time period; cells as in (b), subunits as indicated. \*Statistically significant difference vs. wild-type hMiRP1–Kv2.1 ( $P < 0.05$ )

## Discussion

### Multiple Roles for MinK and MiRP1 in Mammalian Heart

The finding here that MinK and MiRP1 coassemble with Kv2.1  $\alpha$ -subunits in rat heart broadens the possible role of these two *KCNE* subunits in mammalian cardiac physiology. It has long been recognized that MinK–KCNQ1 complexes form  $I_{Ks}$  in mammalian heart (Barhanin et al. 1996; Sanguinetti et al. 1996). Since this discovery, MinK and MiRPs have been found to interact with a wide array of Kv channel  $\alpha$ -subunits expressed in the heart, although formation of native complexes has not been proven for all putative partnerships. Both MinK and MiRP1 are expressed in guinea pig, horse and human heart (Abbott et al. 1999; Bertaso et al. 2002; Jiang et al. 2004; Perea et al. 2000). Our current findings for expression of MinK and MiRP1 in rat heart are consistent with previous reports showing that mRNA for both MinK (Folander et al. 1990; Ohya et al. 2002; Yang et al. 1994) and MiRP1 (Ohya et al. 2002) is expressed in rat heart. Aside from KCNQ1, MinK also modulates ERG (McDonald et al. 1997); and although this association has not been established in human tissue, MinK–ERG complexes were found using coimmunoprecipitation studies in equine heart (Finley et al. 2002) and, here, in rat heart (Fig. 1f). We also previously reported that

*Xenopus laevis* MinK slows Kv2.1 activation in *Xenopus* oocytes (Gordon et al. 2006).

Using a *kcne2* null mouse line, we recently found that MiRP1 forms complexes with Kv1.5 and with Kv4.2 in adult murine ventricles but not with Kv2.1 (Roepke et al. 2008). Native current recordings supported these findings and, together with our present data, demonstrate that expression in a tissue of two subunits capable of interaction does not necessarily confirm their native interaction. Likewise, in the present study we found that, despite expression in rat heart, MiRP2 does not form stable complexes with Kv2.1 in rat heart, contrasting with our previous finding that MiRP2 forms stable complexes with Kv2.1 in rat brain (McCrossan et al. 2003). Further, the contrasting findings in the rat and mouse heart highlight the necessity to understand the limitations of studying a single model system, although we have yet to study murine atria; thus, it is possible that MiRP1–Kv2.1 complexes exist there.

MiRP1 modulates hERG function and pharmacology, and MiRP1–hERG complexes may contribute to generating  $I_{Kr}$  in human heart (Abbott et al. 1999). Throughout rat heart development MiRP1 strongly colocalizes with rERG (Chun et al. 2004), consistent with our data here suggesting formation of MiRP1–rERG complexes in rat heart (Fig. 1f). Further, in a canine model of cardiac disease, MiRP1 upregulation was recently shown to reduce  $I_{Kr}$  (Jiang et al. 2004), as would be expected if the two coassemble in canine heart because MiRP1 lowers the unitary conductance of ERG (Abbott et al. 1999). MiRP2 also suppresses hERG currents in *Xenopus* oocyte expression experiments (Abbott et al. 2001; Anantharam et al. 2003; Han et al. 2002; Lewis et al. 2004; McCrossan et al. 2003; Schroeder et al. 2000). While the expression of MiRP2 in heart tissue suggests a role in cardiac excitability, it is not yet known whether MiRP2 modulates hERG, KCNQ1 or any other channels in vivo in mammalian heart.

### Cardiac Effects of Genetic Disruption of MinK and MiRP1

Cardiac expression, demonstration of the ability to modulate specific cardiac channels in heterologous systems and native cardiac coimmunoprecipitations all offer evidence supporting specific roles for MinK and MiRP1 in cardiac physiology. Genetic evidence provides perhaps stronger evidence in support of roles for MinK and MiRP1 in the heart, but what can it tell us about specific partnerships? MinK knockout was previously reported to induce only a mild cardiac phenotype (Charpentier et al. 1998), but the profound sensorineural deafness exhibited by MinK null mice (and KCNQ1 null mice) (Lee et al. 2000; Vetter et al. 1996) is consistent with an association of MinK mutations

with Jervell and Lange-Nielsen syndrome (JLNS), an inherited human disorder that presents as LQTS and deafness (Splawski et al. 1997a, b; Tyson et al. 1997). The disruption of potassium secretion into the endolymph of the inner ear in JLNS by knockout or mutation of MinK is accepted to be due to dysfunction of MinK–KCNQ1 complexes in the ear, especially as KCNQ1 mutations can also cause JLNS (Schulze-Bahr et al. 1997; Tyson et al. 1997), but the LQTS component could be also caused by dysfunction of other channels that MinK may associate with in the heart, including ERG (Bianchi et al. 1999; McDonald et al. 1997). Recently, MinK null mice were also found to exhibit atrial fibrillation (Temple et al. 2005), and a MinK polymorphism was previously found to be enriched in human atrial fibrillation patients compared to control subjects (Lai et al. 2002). Despite the fact that MinK increases KCNQ1 unitary and macroscopic conductance approximately fourfold, MinK knockout increased  $I_K$  current in atrial myocytes; interestingly, this was not exclusively due to upregulation of currents sensitive to chromanol 293, a KCNQ1 and  $I_{Ks}$  blocker (Temple et al. 2005). Our present findings provide a possible explanation for this: If MinK–Kv2.1 currents form in murine atrium as they do in rat heart, then MinK knockout would be expected to upregulate atrial  $I_K$  (provided mouse MinK, like rat MinK, reduces Kv2.1 current density). Our present study in rat heart might also help to explain the previously observed heterogeneity in Kv2.1 current magnitude and kinetics isolated from the mid-myocardial left ventricular wall (Schultz et al. 2001). There, the authors speculate that heteromultimerization with other Kv channel  $\alpha$ -subunits might be a contributing factor; given our results, MinK and MiRP1 interaction should also be considered.

The effects reported here of D76N on human MinK–Kv2.1 function raise the possibility that disruption of MinK–Kv2.1 currents may contribute to D76N-associated disease—the combined effects of the D76N mutation serve to decrease the repolarizing ability of MinK–Kv2.1 complexes, predicted to lengthen the action potential in myocytes in which Kv2.1 is a repolarizing current. The single significant effect of S74L—slowing of hMinK–Kv2.1 deactivation—in contrast, could shorten the action potential by delaying channel closure toward the end of phase 3. However, while Kv2.1 is expressed in human heart, its role in human cardiac repolarization is not yet known. Its expression is likely much lower in human heart than that of hERG and KCNQ1; therefore, its role in human cardiac repolarization is probably less significant.

Mutations and polymorphisms in MiRP1, including M54T and I57T, reduce MiRP1–hERG currents and are associated with inherited and drug-induced LQTS (Abbott et al. 1999; Isbrandt et al. 2002; Sesti et al. 2000). The R27C variant of MiRP1 is also implicated in atrial

fibrillation and has been shown to increase MiRP1–KCNQ1 currents without affecting MiRP1–hERG or MiRP1–HCN channel function (Yang et al. 2004). M54T and I57T produced reductions of 34–47% in MiRP1–hERG tail current density at  $-40$  mV; M54T–MiRP1–hERG channels activated less readily at a given voltage and deactivated more rapidly than channels formed with wild-type MiRP1 and hERG (Abbott et al. 1999; Sesti et al. 2000). The effects of M54T and I57T on MiRP1–Kv2.1 channels found here—greatly slowed activation and (in the case of M54T) positively shifted voltage dependence of activation—would also be expected to lengthen the action potential of cells requiring MiRP1–Kv2.1 for repolarization. Without a known role for Kv2.1 in human myocytes we cannot speculate further on the potential role of MiRP1–Kv2.1 current disruption in human cardiac pathophysiology. In mice, *kcnj2* knockout prolongs ventricular action potential duration and increases the QT interval under sevoflurane anesthesia, but these effects are almost certainly due to reduced  $I_{K,slow1}$  and  $I_{to,f}$  density due to loss of MiRP1 regulation of Kv1.5 and Kv4.2, respectively (Roepke et al. 2008).

## Conclusions and Limitations

In summary, our data provide evidence for the presence of two novel potassium channel complexes in rat hearts, suggesting a role for MinK–Kv2.1 and MiRP1–Kv2.1 complexes in cardiac physiology. Both MinK and MiRP1 alter Kv2.1 function; mutations in MinK and MiRP1 associated with human LQTS impair function of complexes formed with Kv2.1. Further studies are necessary to determine exactly when and where in the heart these complexes form and how important regulation of Kv2.1 by MinK or MiRP1 is to the generation of  $I_K$  in the hearts of rats and other species. These studies may be hampered if the lack of effect of MinK or MiRP1 on Kv2.1 sensitivity to TEA is also observed with other pharmacological tools, and ultimately a combination of genetic evidence and regional native electrophysiology studies may be necessary to pin down roles for MinK–Kv2.1 and MiRP1–Kv2.1 complexes in specific cardiac regions or cell types. Further studies are also required to determine which of the sequence differences between the rat and human forms of MinK and MiRP1 (29/129 and 22/123 residues, respectively) give rise to their functional differences. No obvious patterns emerge from examination of these sequences, except that the transmembrane domains differ the least between rat and human in each case (one or two residues), with the rest of the variant residues scattered throughout the extracellular and intracellular domains (Abbott and Goldstein 1998).

An extensive diversity of Kv channel subunit expression has been identified between atria and ventricles, and Kv channel subunits are also differentially expressed in circumscribed regions in the left ventricular wall, between endo- and epicardial regions and in distinct areas of the conduction system as well as in the aging and diseased heart (Dixon and McKinnon 1994; Jiang et al. 2004; Pourrier et al. 2003; Schultz et al. 2001). Kv2.1 is expressed highly in rat heart atria and to a lesser extent in rat ventricles; MinK and MiRP1 are expressed in rat heart (Fig. 1), in murine atria and SA and AV nodes and in human, horse and guinea pig atria and ventricles (Barry et al. 1995; Finley et al. 2002; Jiang et al. 2004; Szabo et al. 2005; Warth and Barhanin 2002). Additionally, MiRP1 expression is upregulated in aging and downregulated in ischemic rat hearts (Jiang et al. 2004), and both MinK and MiRP1 are reportedly highly expressed in canine Purkinje fibers (Pourrier et al. 2003).

It becomes apparent that the task of identifying specific MiRP- $\alpha$ -subunit partnerships and their native current correlates is a monumental one that will require concerted biochemical, pharmacological and genetic analyses at the subtissue level in a range of species; the present study essentially offers a starting point for analysis of Kv2.1 complexes. This task may ultimately prove futile in some cases if MiRPs provide a mechanism for dynamically modulating channel function as opposed to providing an expanded but defined range of currents in combination with a finite number of different  $\alpha$ -subunits. We previously found that interactions of MinK, MiRP1 and MiRP2 increase the functional diversity of the Kv3 family delayed rectifiers, broadening their potential role outside that of sustaining rapid firing in neurons (Lewis et al. 2004). We now find that Kv2.1 is also differentially modulated by MinK, MiRP1 and (previously) MiRP2 (McCrossan et al. 2003); but we are no closer to understanding exactly how all these possible combinations are utilized in native tissue. A recent quantitative RT-PCR analysis showed differential mRNA expression for all five MiRPs across the right and left atria and ventricles of human heart and increased expression in cardiomyopathy (Lundquist et al. 2005). In the same study, CHO cell expression experiments showed that MinK prevented modulation of KCNQ1 by MiRP1 but that MiRPs 2–4 could override the effects of MinK on KCNQ1—thus, KCNQ1 may be modulated by multiple MiRPs in human heart depending on subtissue or even subcellular distribution and other temporal or regulatory factors. Now that we understand that both MiRPs and  $\alpha$ -subunits exhibit promiscuous partnering, future studies are warranted to examine how spatial and temporal variation in cardiac expression levels of MiRPs and Kv channel  $\alpha$ -subunits impacts complex formation, native current properties and action potential duration and refractoriness

in different regions of the heart in humans and in animal models.

**Acknowledgements** G. W. A. is grateful for support from the National Institutes of Health (R01 HL079275) and the American Heart Association (grant-in-aid 0855756D). We thank Dr. Sandra Chaplan for assistance with antibody development, Stephanie Backovic for help with protein immunochemistry and Dr. Daniel J. Lerner for insightful comments on the manuscript.

## References

- Abbott GW, Goldstein SA (1998) A superfamily of small potassium channel subunits: form and function of the MinK-related peptides (MiRPs). *Q Rev Biophys* 31:357–398
- Abbott GW, Sesti F, Splawski I, Buck ME, Lehmann MH, Timothy KW, Keating MT, Goldstein SA (1999) MiRP1 forms IKr potassium channels with HERG and is associated with cardiac arrhythmia. *Cell* 97:175–187
- Abbott GW, Butler MH, Bendahhou S, Dalakas MC, Ptacek LJ, Goldstein SA (2001) MiRP2 forms potassium channels in skeletal muscle with Kv3.4 and is associated with periodic paralysis. *Cell* 104:217–231
- Anantharam A, Lewis A, Panaghie G, Gordon E, McCrossan ZA, Lerner DJ, Abbott GW (2003) RNA interference reveals that endogenous *Xenopus* MinK-related peptides govern mammalian K<sup>+</sup> channel function in oocyte expression studies. *J Biol Chem* 278:11739–11745
- Antonucci DE, Lim ST, Vassanelli S, Trimmer JS (2001) Dynamic localization and clustering of dendritic Kv2.1 voltage-dependent potassium channels in developing hippocampal neurons. *Neuroscience* 108:69–81
- Barhanin J, Lesage F, Guillemare E, Fink M, Lazdunski M, Romey G (1996) K(V)LQT1 and IsK (minK) proteins associate to form the I(Ks) cardiac potassium current. *Nature* 384:78–80
- Barry DM, Trimmer JS, Merlie JP, Nerbonne JM (1995) Differential expression of voltage-gated K<sup>+</sup> channel subunits in adult rat heart. Relation to functional K<sup>+</sup> channels? *Circ Res* 77:361–369
- Bertaso F, Sharpe CC, Hendry BM, James AF (2002) Expression of voltage-gated K<sup>+</sup> channels in human atrium. *Basic Res Cardiol* 97:424–433
- Bianchi L, Shen Z, Dennis AT, Priori SG, Napolitano C, Ronchetti E, Byskin R, Schwartz PJ, Brown AM (1999) Cellular dysfunction of LQT5-minK mutants: abnormalities of IKs, IKr and trafficking in long QT syndrome. *Hum Mol Genet* 8:1499–1507
- Bou-Abboud E, Nerbonne JM (1999) Molecular correlates of the calcium-independent, depolarization-activated K<sup>+</sup> currents in rat atrial myocytes. *J Physiol* 517(Pt 2):407–420
- Bou-Abboud E, Li H, Nerbonne JM (2000) Molecular diversity of the repolarizing voltage-gated K<sup>+</sup> currents in mouse atrial cells. *J Physiol* 529(Pt 2):345–358
- Capuano V, Ruchon Y, Antoine S, Sant MC, Renaud JF (2002) Ventricular hypertrophy induced by mineralocorticoid treatment or aortic stenosis differentially regulates the expression of cardiac K<sup>+</sup> channels in the rat. *Mol Cell Biochem* 237:1–10
- Charpentier F, Merot J, Riochet D, Le Marec H, Escande D (1998) Adult KCNE1-knockout mice exhibit a mild cardiac cellular phenotype. *Biochem Biophys Res Commun* 251:806–810
- Chen YH, Xu SJ, Bendahhou S, Wang XL, Wang Y, Xu WY, Jin HW, Sun H, Su XY, Zhuang QN, Yang YQ, Li YB, Liu Y, Xu HJ, Li XF, Ma N, Mou CP, Chen Z, Barhanin J, Huang W (2003) KCNQ1 gain-of-function mutation in familial atrial fibrillation. *Science* 299:251–254



- Chun KR, Koenen M, Katus HA, Zehelein J (2004) Expression of the IKr components KCNH2 (rERG) and KCNE2 (rMiRP1) during late rat heart development. *Exp Mol Med* 36:367–371
- Conforti L, Millhorn DE (1997) Selective inhibition of a slow-inactivating voltage-dependent K<sup>+</sup> channel in rat PC12 cells by hypoxia. *J Physiol* 502(Pt 2):293–305
- Dixon JE, McKinnon D (1994) Quantitative analysis of potassium channel mRNA expression in atrial and ventricular muscle of rats. *Circ Res* 75:252–260
- Du J, Tao-Cheng JH, Zerfas P, McBain CJ (1998) The K<sup>+</sup> channel, Kv2.1, is apposed to astrocytic processes and is associated with inhibitory postsynaptic membranes in hippocampal and cortical principal neurons and inhibitory interneurons. *Neuroscience* 84:37–48
- Finley MR, Li Y, Hua F, Lillich J, Mitchell KE, Ganta S, Gilmour RF Jr, Freeman LC (2002) Expression and coassociation of ERG1, KCNQ1, and KCNE1 potassium channel proteins in horse heart. *Am J Physiol* 283:H126–H138
- Folander K, Smith JS, Antanavage J, Bennett C, Stein RB, Swanson R (1990) Cloning and expression of the delayed-rectifier IsK channel from neonatal rat heart and diethylstilbestrol-primed rat uterus. *Proc Natl Acad Sci USA* 87:2975–2979
- Frech GC, VanDongen AM, Schuster G, Brown AM, Joho RH (1989) A novel potassium channel with delayed rectifier properties isolated from rat brain by expression cloning. *Nature* 340:642–645
- Gordon E, Roepke TK, Abbott GW (2006) Endogenous KCNE subunits govern Kv2.1 K<sup>+</sup> channel activation kinetics in *Xenopus* oocyte studies. *Biophys J* 90:1223–1231
- Han W, Bao W, Wang Z, Nattel S (2002) Comparison of ion-channel subunit expression in canine cardiac Purkinje fibers and ventricular muscle. *Circ Res* 91:790–797
- Huang B, Qin D, El-Sherif N (2001) Spatial alterations of Kv channels expression and K<sup>+</sup> currents in post-MI remodeled rat heart. *Cardiovasc Res* 52:246–254
- Isbrandt D, Friederich P, Solth A, Haverkamp W, Ebneith A, Borggreffe M, Funke H, Sauter K, Breithardt G, Pongs O, Schulze-Bahr E (2002) Identification and functional characterization of a novel KCNE2 (MiRP1) mutation that alters HERG channel kinetics. *J Mol Med* 80:524–532
- Jiang M, Zhang M, Tang DG, Clemo HF, Liu J, Holwitt D, Kasirajan V, Pond AL, Wettwer E, Tseng GN (2004) KCNE2 protein is expressed in ventricles of different species, and changes in its expression contribute to electrical remodeling in diseased hearts. *Circulation* 109:1783–1788
- Kaab S, Dixon J, Duc J, Ashen D, Nabauer M, Beuckelmann DJ, Steinbeck G, McKinnon D, Tomaselli GF (1998) Molecular basis of transient outward potassium current downregulation in human heart failure: a decrease in Kv4.3 mRNA correlates with a reduction in current density. *Circulation* 98:1383–1393
- Kuryshev YA, Gudzh TI, Brown AM, Wible BA (2000) KChAP as a chaperone for specific K<sup>+</sup> channels. *Am J Physiol* 278:C931–C941
- Lai LP, Su MJ, Yeh HM, Lin JL, Chiang FT, Hwang JJ, Hsu KL, Tseng CD, Lien WP, Tseng YZ, Huang SK (2002) Association of the human minK gene 38G allele with atrial fibrillation: evidence of possible genetic control on the pathogenesis of atrial fibrillation. *Am Heart J* 144:485–490
- Le Bouter S, Demolombe S, Chambellan A, Bellocq C, Aimond F, Toumaniantz G, Lande G, Siavoshian S, Baro I, Pond AL, Nerbonne JM, Leger JJ, Escande D, Charpentier F (2003) Microarray analysis reveals complex remodeling of cardiac ion channel expression with altered thyroid status: relation to cellular and integrated electrophysiology. *Circ Res* 92:234–242
- Lee MP, Ravenel JD, Hu RJ, Lustig LR, Tomaselli G, Berger RD, Brandenburg SA, Litzi TJ, Bunton TE, Limb C, Francis H, Gorelikow M, Gu H, Washington K, Argani P, Goldenring JR, Coffey RJ, Feinberg AP (2000) Targeted disruption of the *Kvlqt1* gene causes deafness and gastric hyperplasia in mice. *J Clin Invest* 106:1447–1455
- Lewis A, McCrossan ZA, Abbott GW (2004) MinK, MiRP1 and MiRP2 diversify Kv3.1 and Kv3.2 potassium channel gating. *J Biol Chem* 279:2884–2892
- Lundquist AL, Manderfield LJ, Vanoye CG, Rogers CS, Donahue BS, Chang PA, Drinkwater DC, Murray KT, George AL Jr (2005) Expression of multiple KCNE genes in human heart may enable variable modulation of I(Ks). *J Mol Cell Cardiol* 38:277–287
- McCrossan ZA, Abbott GW (2004) The MinK-related peptides. *Neuropharmacology* 47:787–821
- McCrossan ZA, Lewis A, Panaghie G, Jordan PN, Christini DJ, Lerner DJ, Abbott GW (2003) MinK-related peptide 2 modulates Kv2.1 and Kv3.1 potassium channels in mammalian brain. *J Neurosci* 23:8077–8091
- McDonald TV, Yu Z, Ming Z, Palma E, Meyers MB, Wang KW, Goldstein SA, Fishman GI (1997) A minK–HERG complex regulates the cardiac potassium current I(Kr). *Nature* 388:289–292
- Murakoshi H, Trimmer JS (1999) Identification of the Kv2.1 K<sup>+</sup> channel as a major component of the delayed rectifier K<sup>+</sup> current in rat hippocampal neurons. *J Neurosci* 19:1728–1735
- Ohya S, Asakura K, Muraki K, Watanabe M, Imaizumi Y (2002) Molecular and functional characterization of ERG, KCNQ, and KCNE subtypes in rat stomach smooth muscle. *Am J Physiol* 282:G277–G287
- Pereon Y, Demolombe S, Baro I, Drouin E, Charpentier F, Escande D (2000) Differential expression of KvLQT1 isoforms across the human ventricular wall. *Am J Physiol* 278:H1908–H1915
- Piccini M, Vitelli F, Seri M, Galletta LJ, Moran O, Bulfone A, Banfi S, Pober B, Renieri A (1999) KCNE1-like gene is deleted in AMME contiguous gene syndrome: identification and characterization of the human and mouse homologs. *Genomics* 60:251–257
- Pitts BJ (1979) Stoichiometry of sodium–calcium exchange in cardiac sarcolemmal vesicles. Coupling to the sodium pump. *J Biol Chem* 254:6232–6235
- Post MA, Kirsch GE, Brown AM (1996) Kv2.1 and electrically silent Kv6.1 potassium channel subunits combine and express a novel current. *FEBS Lett* 399:177–182
- Pourrier M, Zicha S, Ehrlich J, Han W, Nattel S (2003) Canine ventricular KCNE2 expression resides predominantly in Purkinje fibers. *Circ Res* 93:189–191
- Roepke TK, Kontogeorgis A, Ovanez C, Xu X, Young JB, Purtell K, Goldstein PA, Christini DJ, Peters NS, Akar FG, Gutstein DE, Lerner DJ, Abbott GW (2008) Targeted deletion of *kcne2* impairs ventricular repolarization via disruption of I(K, slow1) and I(to, f). *FASEB J* 22:3648–3660
- Salinas M, de Weille J, Guillemare E, Lazdunski M, Hugnot JP (1997a) Modes of regulation of shab K<sup>+</sup> channel activity by the Kv8.1 subunit. *J Biol Chem* 272:8774–8780
- Salinas M, Duprat F, Heurteaux C, Hugnot JP, Lazdunski M (1997b) New modulatory alpha subunits for mammalian Shab K<sup>+</sup> channels. *J Biol Chem* 272:24371–24379
- Sanguinetti MC, Curran ME, Zou A, Shen J, Spector PS, Atkinson DL, Keating MT (1996) Coassembly of K(V)LQT1 and minK (IsK) proteins to form cardiac I(Ks) potassium channel. *Nature* 384:80–83
- Schroeder BC, Waldegger S, Fehr S, Bleich M, Warth R, Greger R, Jentsch TJ (2000) A constitutively open potassium channel formed by KCNQ1 and KCNE3. *Nature* 403:196–199
- Schultz JH, Volk T, Ehmke H (2001) Heterogeneity of Kv2.1 mRNA expression and delayed rectifier current in single isolated myocytes from rat left ventricle. *Circ Res* 88:483–490
- Schulze-Bahr E, Haverkamp W, Wedekind H, Rubie C, Hordt M, Borggreffe M, Assmann G, Breithardt G, Funke H (1997)



- Autosomal recessive long-QT syndrome (Jervell Lange-Nielsen syndrome) is genetically heterogeneous. *Hum Genet* 100: 573–576
- Sesti F, Goldstein SA (1998) Single-channel characteristics of wild-type IKs channels and channels formed with two minK mutants that cause long QT syndrome. *J Gen Physiol* 112:651–663
- Sesti F, Abbott GW, Wei J, Murray KT, Saksena S, Schwartz PJ, Priori SG, Roden DM, George AL Jr, Goldstein SA (2000) A common polymorphism associated with antibiotic-induced cardiac arrhythmia. *Proc Natl Acad Sci USA* 97:10613–10618
- Splawski I, Timothy KW, Vincent GM, Atkinson DL, Keating MT (1997a) Molecular basis of the long-QT syndrome associated with deafness. *N Engl J Med* 336:1562–1567
- Splawski I, Tristani-Firouzi M, Lehmann MH, Sanguinetti MC, Keating MT (1997b) Mutations in the hminK gene cause long QT syndrome and suppress IKs function. *Nat Genet* 17:338–340
- Szabo G, Szentandrassy N, Biro T, Toth BI, Czifra G, Magyar J, Banyasz T, Varro A, Kovacs L, Nanasi PP (2005) Asymmetrical distribution of ion channels in canine and human left-ventricular wall: epicardium versus midmyocardium. *Pfluegers Arch* 450: 307–316
- Temple J, Frias P, Rottman J, Yang T, Wu Y, Verheijck EE, Zhang W, Siprachanh C, Kanki H, Atkinson JB, King P, Anderson ME, Kupersmidt S, Roden DM (2005) Atrial fibrillation in KCNE1-null mice. *Circ Res* 97:62–69
- Tyson J, Tranebjaerg L, Bellman S, Wren C, Taylor JF, Bathen J, Aslaksen B, Sorland SJ, Lund O, Malcolm S, Pembrey M, Bhattacharya S, Bitner-Glindzicz M (1997) IsK and KvLQT1: mutation in either of the two subunits of the slow component of the delayed rectifier potassium channel can cause Jervell and Lange-Nielsen syndrome. *Hum Mol Genet* 6:2179–2185
- Van Wagoner DR, Pond AL, McCarthy PM, Trimmer JS, Nerbonne JM (1997) Outward K<sup>+</sup> current densities and Kv1.5 expression are reduced in chronic human atrial fibrillation. *Circ Res* 80: 772–781
- Vetter DE, Mann JR, Wangemann P, Liu J, McLaughlin KJ, Lesage F, Marcus DC, Lazdunski M, Heinemann SF, Barhanin J (1996) Inner ear defects induced by null mutation of the *isk* gene. *Neuron* 17:1251–1264
- Warth R, Barhanin J (2002) The multifaceted phenotype of the knockout mouse for the KCNE1 potassium channel gene. *Am J Physiol* 282:R639–R648
- Xu C, Lu Y, Tang G, Wang R (1999a) Expression of voltage-dependent K<sup>+</sup> channel genes in mesenteric artery smooth muscle cells. *Am J Physiol* 277:G1055–G1063
- Xu H, Barry DM, Li H, Brunet S, Guo W, Nerbonne JM (1999b) Attenuation of the slow component of delayed rectification, action potential prolongation, and triggered activity in mice expressing a dominant-negative Kv2 alpha subunit. *Circ Res* 85: 623–633
- Yang T, Wathen MS, Felipe A, Tamkun MM, Snyders DJ, Roden DM (1994) K<sup>+</sup> currents and K<sup>+</sup> channel mRNA in cultured atrial cardiac myocytes (AT-1 cells). *Circ Res* 75:870–878
- Yang Y, Xia M, Jin Q, Bendahhou S, Shi J, Chen Y, Liang B, Lin J, Liu Y, Liu B, Zhou Q, Zhang D, Wang R, Ma N, Su X, Niu K, Pei Y, Xu W, Chen Z, Wan H, Cui J, Barhanin J, Chen Y (2004) Identification of a KCNE2 gain-of-function mutation in patients with familial atrial fibrillation. *Am J Hum Genet* 75:899–905